Role of Different Regions of α-Synuclein in the Assembly of Fibrils†

Zhijie Qin,[#] Dongmei Hu,[#] Shubo Han,[§] Dong-Pyo Hong,[#] and Anthony L. Fink*,[#]

Department of Chemistry & Biochemistry, University of California, Santa Cruz California 95064, and Department of Natural Sciences, Fayetteville State University, Fayetteville, North Carolina 28301

Received July 17, 2007; Revised Manuscript Received September 5, 2007

ABSTRACT: Elucidating the details of the assembly of amyloid fibrils is a key step to understanding the mechanism of amyloid deposition diseases including Parkinson's disease. Although several models have been proposed, based on analyses of polypeptides and short peptides, a detailed understanding of the structure and mechanism of α-synuclein fibrillation remains elusive. In this study, we used trypsin and endoproteinase GluC to digest intact α-synuclein fibrils and to analyze the detailed morphology of the resultant fibrils/remnants. We also created three mutants of α-synuclein, in which the N-terminal and C-terminal regions were removed, both individually and in combination, and investigated the detailed morphology of the fibrils from these mutants. Our results indicate that the assembly of mature α-synuclein fibrils is hierarchical: protofilaments → protofibrils → mature fibrils. There is a core region of ∼70 amino acids, from residues ∼32 to 102, which comprises the β-rich core of the protofilaments and fibrils. In contrast, the two terminal regions show no evidence of participating in the assembly of the protofilament core but play a key role in the interactions between the protofilaments, which is necessary for the fibril maturation.

Parkinson's disease is predominantly a movement disorder resulting from the degeneration of dopaminergic neurons in the substantia nigra. The cause of the disease is unknown, but substantial evidence suggests that the aggregation of α-synuclein is a critical step in the etiology of Parkinson's disease (PD)[1] (*1*). In patients with Parkinson's disease, fibrils of α-synuclein are observed in Lewy bodies, the cardinal hallmark of PD pathology (*2*). Linkage studies have shown that three independent missense mutations (A30P, E46K, and A53T) within the α-synuclein gene lead to rare familial forms of early onset PD (*3*−*5*); familial early onset PD is also caused by overexpression of α-synuclein due to duplication or triplication of the α-synuclein gene locus (*6*−*10*). The production of wild-type (WT) α-synuclein in transgenic mice or of WT or the familial variants A30P and A53T in transgenic flies leads to motor deficits and neuronal inclusions reminiscent of PD (*11*−*13*).

α-Synuclein is an abundant brain protein of 140 residues, lacking both cysteine and tryptophan residues. A variety of spectroscopic studies, including NMR, indicate that α-synuclein is an intrinsically disordered protein (*14*−*17*). α-Synuclein is present in high concentration at presynaptic terminals and is found in both soluble and membrane-associated fractions of the brain. Several possible functions have been suggested, and it appears to be involved in vesicle release and trafficking. Although α-synuclein is intrinsically unstructured when free in solution, it undergoes a structural transition to a highly helical state in the presence of either brain-derived or synthetic lipid vesicles (*18*, *19*), and theoretical sequence prediction also indicates the propensity for helix formation. In the fibril form, the protein assumes a cross-β structure (*20*, *21*), in which individual β-strands are perpendicular to the fibril axis.

The structure of α-synuclein can be divided into three regions: residues 1−60, which contain four 11-amino acid imperfect repeats (coding for amphipathic helices) with a consensus motif (KTKEGV), residues 61−95, which contain the amyloidogenic NAC region (*22*) and two additional repeats, and the highly charged C-terminal region, residues 96−140. NAC (nonamyloid β component of Alzheimer's disease amyloid) is a 35-amino acid fragment of α-synuclein originally isolated from brain tissue of Alzheimer's disease patients (*23*), which comprises the hydrophobic core of the protein and has been shown to have a key role in fibrillation (*22*). More recent studies showed that even shorter peptides from the NAC region can form fibrils (*24*, *25*). However, fibril structure studies using site-directed spin labeling (*26*), proteinase K digestion (*27*), solid-state NMR (*28*), and H/D exchange (*29*) suggest that the core region of α-synuclein involved in the fibril core is longer, around 70 amino acids.

In order to determine the roles of the three regions of α-synuclein in assembly of the fibrils, we performed protease digestion studies on the intact fibrils of α-synuclein using two distinct proteases, trypsin and endoproteinase GluC, and analyzed the detailed morphologies of the resultant fibrils/remnants, as well as their molecular masses. On the basis of the results, we created three truncated α-synucleins: Syn30−140, the truncation of residues 1−29 from α-synuclein, Syn1−103, the truncation of residues 104−140 from α-synuclein, and Syn30−103, which is the double terminal

† Supported by grant NS39985 from the National Institutes of Health.

* Corresponding author. Tel: (831) 459-2744, fax: (831) 459-2935; e-mail: enzyme@cats.ucsc.edu.

[#] University of California, Santa Cruz.

[§] Fayetteville State University.

[1] Abbreviations: PD, Parkinson's disease; AFM, atomic force microscopy; ATR FTIR, attenuated total reflectance Fourier transform infrared spectroscopy.

10.1021/bi7014053 CCC: $37.00 © 2007 American Chemical Society
Published on Web 10/27/2007

truncation of N- and C-termini. Fibrils from these three truncations were obtained, and their morphology was analyzed using atomic force microscopy (AFM). Our findings show that the assembly of the mature fibrils is hierarchical. There is a region of ~70 amino acids from residue 32 to 102, which is involved in the assembly of the β-rich core of the protofilaments. The two terminal regions show no evidence of participating in the assembly of the protofilament core but play a role in the interactions between protofilaments, which is necessary for the fibril maturation.

MATERIALS AND METHODS

Sample Preparation. Human wild type α-synuclein was expressed in the *E. coli* BL21(DE3) cell line transformed with pRK172/ α-synuclein WT plasmid (kind gift of M. Goedert, MRC Cambridge) and purified as previously described (*30*). The mutants of Syn30−140, Syn1−103, and Syn30−103 were created using the QuikChange site-directed mutagenesis protocol (Stratagene). The procedure for Syn30−140 purification was the same as for WT α-synuclein. A modified procedure was used for Syn1−103 and Syn30−103 purification, mainly using cation ion-exchange chromatography (Hitrap SP FF 5 mL, Pharmacia) in place of the anion-exchange chromatography. The resultant α-synuclein proteins were judged to be >95% pure following SDS-polyacrylamide electrophoresis, gel-filtration, and MS analysis.

To make fibrils, the lyophilized powder of wild type α-synuclein, Syn30−140, and Syn1−103 were dissolved in phosphate buffer (10 mM, pH 7.4) and airfuged (Beckman) at 126 000*g* for 30 min to remove any aggregates. The Syn30−103 was used directly from its fresh prepared solution with airfuge treatment under the same condition. Solutions (0.5 mL) containing 2 mg/mL protein in 10 mM phosphate buffer at pH 7.4 with 100 mM NaCl were incubated at 37 °C with stirring at 600 rpm. The fibrillation was monitored by the thioflavin T assay (*31*) until fibrillation plateaued. The solutions were then collected and centrifuged at 14 000 rpm. The pellets were rinsed with phosphate buffer three times and resuspended in same buffer for further analysis.

Limited Proteolysis of Fibrils. A suspension of fibrils (200 μL) with protein concentration of 2 mg/mL was mixed with trypsin (40 μg/mL) or endoproteinase GluC (100 μg/mL) to reach an 800:1 molar ratio (fibril:enzyme). The mixtures were incubated at 25 °C with gentle shaking. Mass spectrometry analysis was performed at discrete time points to monitor the digestion process. The digestion was halted by spinning down and rinsing the remnants of the fibrils when the mass spectra showed no changes after 2 h of digestion. The insoluble remnants of the fibril digestion were resuspended in phosphate buffer for further analysis.

Mass Spectrometry (MS). An electrospray ionization MS (MicroMass ZMD, UK) mass spectrometer was used to obtain mass spectra. Samples for MS analysis were made by loading 10 μL of the fibril suspension on a mini reverse-phase column (C8, Analytichem International) and eluted using 200 μL of 80% (v/v) aqueous acetonitrile with 1% formic acid. The data was analyzed using MassLynx.

AFM Measurements. Aliquots of 10 μL of fibril suspensions (resuspended insoluble fraction) with 1 M NaCl were placed on the surface of freshly cleaved mica and air-dried. The sample surface was rinsed with flow water for 1 min to remove salts. AFM images were collected with a PicoScan LE SPM system (Molecular Imaging, Phoenix, AZ) equipped with Acoustic AC mode (tapping mode) for *ex situ* experiments. The magnetically coated probes, with a typical 5−7 nm radius and 2.8 N/m spring constant, Type II MAC Levers (Molecular Imaging), were used in MAC mode and oscillated at about 30-kHz resonance frequency under an alternating magnetic field. Triangular cantilevers with 100 kHz resonance frequency and 2 N/m spring constant, the V-shaped cantilever CSC21/Si3N4/No Al (MikroMasch), were used in tapping mode imaging. Heights ranging from 0.1 to 100 nm were estimated by section analysis, and lateral sizes were calibrated with standard calibration grid and gold microspheres. At least four regions of the mica surface were examined to verify that similar structures existed through the sample. No filter treatment was used to modify the images. SPIP 4.0 (Image Metrology) was used to analyze the height, area, and volume distribution.

ATR-FTIR Spectra. FTIR spectra of α-synuclein solution were recorded using a ThermoNicolet Nexus 670 FTIR spectrophotometer in the amide I region from 1700 to 1600 cm^{-1}. A 10 μL amount of each fibril suspension (resuspended insoluble fraction) was applied evenly to the surface of a germanium crystal and dried to form a hydrated thin film by flowing a nitrogen stream across the surface. Background and water vapor subtractions were performed. Peak positions were determined by FSD and second-derivative deconvolution. Curve fitting of the amide I regions (raw spectra) was performed using Gaussian/Lorentzian functions. The areas under the curves were normalized for comparisons.

RESULTS

The Core Region of α-Synuclein Fibrils. To elucidate the structure of the core of α-synuclein fibrils and the solvent-exposed regions, two proteases with different cleavage recognition sites were used to treat the full-length mature α-synuclein fibrils with limited digestion. Trypsin is specific to lysine and arginine, while endoproteinase GluC (*Staphylococcus aureus* Protease V8) selectively cleaves peptide bonds C-terminal to glutamic acid residues (and aspartic acid residues 100−300 times slower than glutamic acid residues). The proteinase-treated fibrils were solubilized and then analyzed with mass spectrometry. Figure 1 shows the mass spectra of the fibrils digested by trypsin (A) and GluC (B), respectively. The peaks in the mass spectra represent the peptides from those regions of the fibrils that were inaccessible to the proteases, i.e., the fibril core. The molecular masses corresponding to peptides and their sites of cleavage are analyzed and summarized in Table 1.

In the case of trypsin digestion, the highest peak has a mass of 10 188 Da, which corresponds to the peptide from residues 1 to 102, and reflects the removal of the C-terminal fragment residues 103−140. This indicates that the C-terminal region is accessible to trypsin and thus located on the surface of the fibrils or protruding from the core. Much smaller peaks of 12 266 and 12 038 Da were observed; these represent the removal of residues 1−21 and 1−23, respectively, indicating that the residues K22 and K24 are also accessible to trypsin in the fibrils. This observation provides

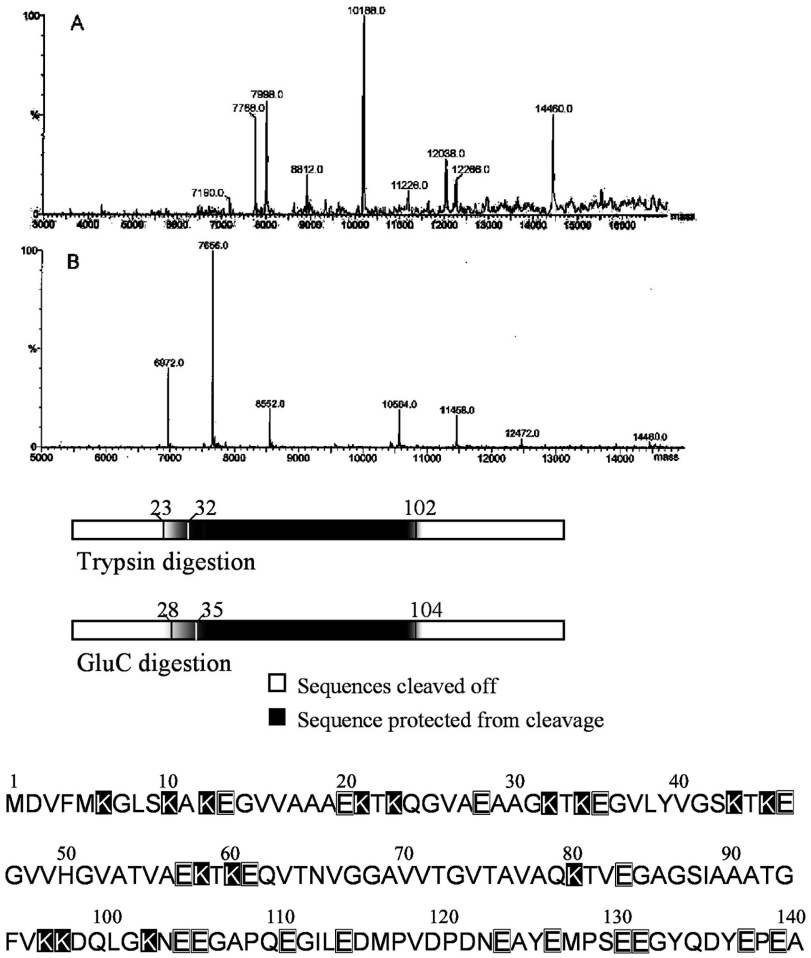

FIGURE 1: The core of α-synuclein fibrils. Mass spectra of α-synuclein fibrils after limited digestion by trypsin (A) and GluC (B). The presence of some intact fibrils is shown by the peak at 14 460 Da, while the other peaks correspond to peptides protected from digestion. The sites of cleavage and the protected peptide segment corresponding to the molecular mass for each peak are summarized in Table 1. From analysis of the MS data, the protected fragments of α-synuclein fibrils are shown below the mass spectra. The sequence of α-synuclein with the potential trypsin sites highlighted in black, and GluC sites in gray, is shown at the bottom of the figure.

Table 1: Protease-Protected Fragments and Corresponding Cleaved Sites of α-synuclein Fibrils

trypsin digestion		GluC digestion	
peptide (kDa)[a]	cleaving site(s)/(peptide length)	peptide MW (Da)[a]	cleaving site(s)/(peptide length)
14460	−/(1−140)	14460	−/(1−140)
12266	K21/(22−140)	12472	E123/(1−123)
12038	K23/(24−140)	11458	E114/(1−114)
11226	K32/(33−140)	10564	E105/(1−105)
10188	K102/(1−102)	8552	E28, E114/(29−114)
7998	K21, K102/(22−102)	7656	E28, E104/(29−104)
7768	K23, K102/(24−102)	6972	E35, E104/(36−104)
8912	?		
7190	?		

[a] The data collection resolution was 2 Da; systemic error is ±2 Da.

evidence that both of the terminal regions of α-synuclein are localized at the surface of the fibril core. A small peak of 11 226 Da was also detected, indicating that residue K31 is less readily accessible to trypsin. MS peaks corresponding to two peptides of 7998 and 7788 Da result from cleavage at both N- and C-terminal regions, resulting in peptides corresponding to residues 22−102 and 24−102, respectively.

Digestion of α-synuclein fibrils by GluC gave the peptides shown in Figure 1B and Table 1. The major peptide observed by MS is 7656 Da, which represents residues 29−104, indicating that residues E28 at the N-terminal and E104 at the C-terminal were cleaved in the fibrils, suggesting that both N- and C-terminal regions are solvent exposed. Interestingly, a peak of 6972 Da can also be detected, which corresponds to the peptide 35−104. The presence of this peptide indicates cleavage at E35, which means this residue is still accessible to GluC but much less so than E28. Other peaks observed in the MS come from single-site cleavage of the fibrils, either at the C- or N-terminals, as described in Table 1.

Since residue 34 is a lysine, and is not accessible to trypsin, we presume that the region between residues 33 and 35 is relatively protected to proteases. Combining the data from trypsin and GluC digestion, we conclude that residues ~32

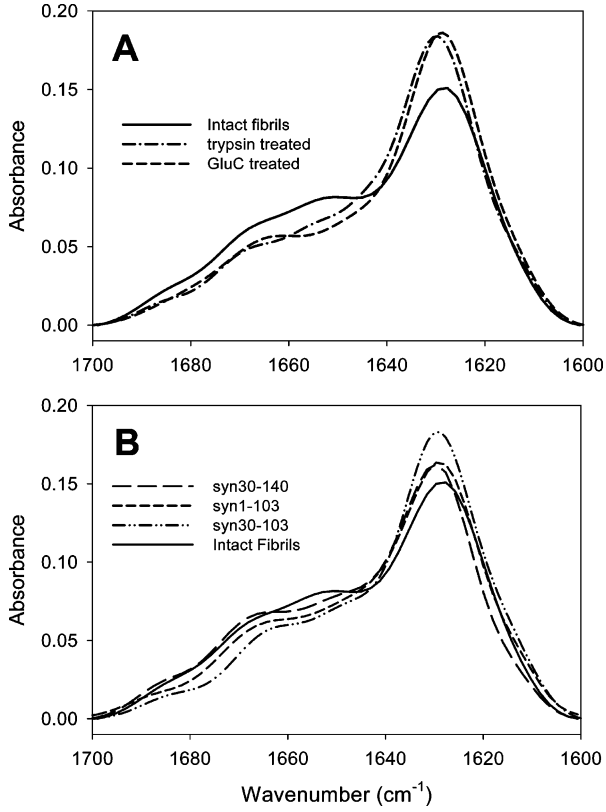

FIGURE 2: Comparison of the secondary structures of different fibrils probed by ATR-FTIR spectra of the amide I region. A, trypsin- (dash) and GluC- (dash dot) digested fibrils compared to intact α-synuclein fibrils (solid). The spectrum of fibrils of full-length α-synuclein (intact fibrils) shows the major peak at 1635 cm^{-1}, reflecting the high content of β-structure. The shoulder around 1650 cm^{-1} represents disordered structure. Compared to the spectrum of fibrils of intact α-synuclein, the spectra of both trypsin- and GluC-treated fibrils show a decrease in absorbance around 1650 cm^{-1} and a large increase in absorbance at ~1635 cm^{-1}, indicating that the protease-digested fibrils have significantly more β-structure and less disordered structure. B, the secondary structure of fibrils from truncated α-synucleins. The increase in absorbance of the 1635 cm^{-1} peaks of the truncated proteins indicate an increase in β-structure, while the decrease at 1650 cm^{-1} reflects less disordered structure compared to intact fibrils. All spectra were normalized to the same area for comparison.

to ~102 of α-synuclein are protected from both of the proteases, forming the core of the fibril, as shown in the diagram in Figure 1.

Secondary Structure of the Fibril Core. ATR-FTIR spectroscopy was used to elucidate the role of two terminal regions in mature fibril assembly and their conformation in the mature fibrils. As shown in Figure 2 A, mature full-length fibrils of α-synuclein are rich in β-structure, characterized by a peak at ~1635 cm^{-1} in the amide I region of the FTIR spectrum. The shoulder at 1650 cm^{-1} represents disordered structure (components >1655 cm^{-1} represent mostly loops and turns). Fibrils digested with both enzymes gave spectra with relatively increased absorbance at 1635 cm^{-1} and decreased absorbance at 1650 cm^{-1}, indicating that removal of the two terminal fragments increases the relative amount of β-structure while decreasing that of disordered structure. These observations suggest that the core fragment (~32 to ~102) of α-synuclein consists of predominantly β-sheet conformation, whereas the N- and C-terminal regions are predominantly disordered and are not part of the fibril core.

To identify the role of different regions along the α-synuclein sequence in the assembly of α-synuclein fibrils, three mutants of truncated α-synuclein (syn30−140, syn1−103, and syn30−103) were produced and their corresponding fibrils were obtained. The secondary structures of the three truncated α-synuclein fibrils were analyzed using ATR-FTIR spectroscopy. As shown in Figure 2B, the FTIR spectrum of syn30−140, the truncated α-synuclein lacking the first 29 residues of the N-terminal region, suggests an increased intensity at 1635 cm^{-1} and decreased absorbance at 1650 cm^{-1} compared with full-length fibrils. This observation indicates that the N-terminal region (residues 1−29) is not involved in the fibril core and has less ordered structural organization. Similarly, the fibrils of the C-terminal truncated protein, syn1−102, also show an increased amount of β-structure and decreased disordered structure. The double truncation, syn30−103 fibrils showed substantially increased β-structure and decreased disordered structure relative to the fibrils of the full-length protein. The data confirm that the C-terminal region of α-syn does not contribute to the ordered structure in fibrils, and that the double-truncated α-synuclein corresponds to the core of α-synuclein fibrils (or protofilaments).

There is very good agreement between the FTIR spectrum of the syn30−103 fibrils with that from the intact fibrils subjected to trypsin and GluC digestion. This suggests that the fibrils of α-synuclein grown from the double truncated mutant (syn30−103) have the same secondary structure as the resistant fragment/core of the protease digested full-length fibrils. This observation confirms that the core of α-synuclein fibrils consists of the region (~32 to ~102), and the two terminal regions of the protein are located outside of the fibril core.

Morphology of Fibrils and Proteolyzed Fibrils. As described above, digestion of α-synuclein fibrils by proteases selectively removes the two terminal regions, leaving the core of the fibril rich in β-structure. To elucidate the morphology of the core of the digested fibrils, AFM images were obtained and their sizes and morphologies analyzed. As shown in Figure 3, the mature full-length fibrils are long and straight, with a periodic twist. The second-derivative image of these fibrils (inset) shows more detail of the twisted structure. The average height of these fibrils was 136.2 ± 6.5 Å (Table 2). In contrast, the protease-resistant fibril core after trypsin digestion shows much thinner filaments aligned in the same direction. The detailed structure of these filaments is shown in the inset to Figure 3. We believe that the uniform alignment of these filaments on the mica is due to solvent flow during sample preparation. The *average* height of the digested fibrils was 27.5 ± 1.6 Å (some heterogeneity in fibril height was observed), less than one-fourth of the size of intact fibrils, and similar to that of protofilaments (see below) (*32*).

To elucidate the role of the two terminal segments in the intact fibrils, we examined the morphology of the fibrils from the three truncated α-synucleins (syn30−140, syn1−103, and syn30−103) (Figure 4). The fibrils of syn30−140, which lack residues 1−29, show straight, long fibrils similar to the morphology of the intact protein. The insets in Figure 4 (upper, enlarged single fibril; lower, second-derivative image)

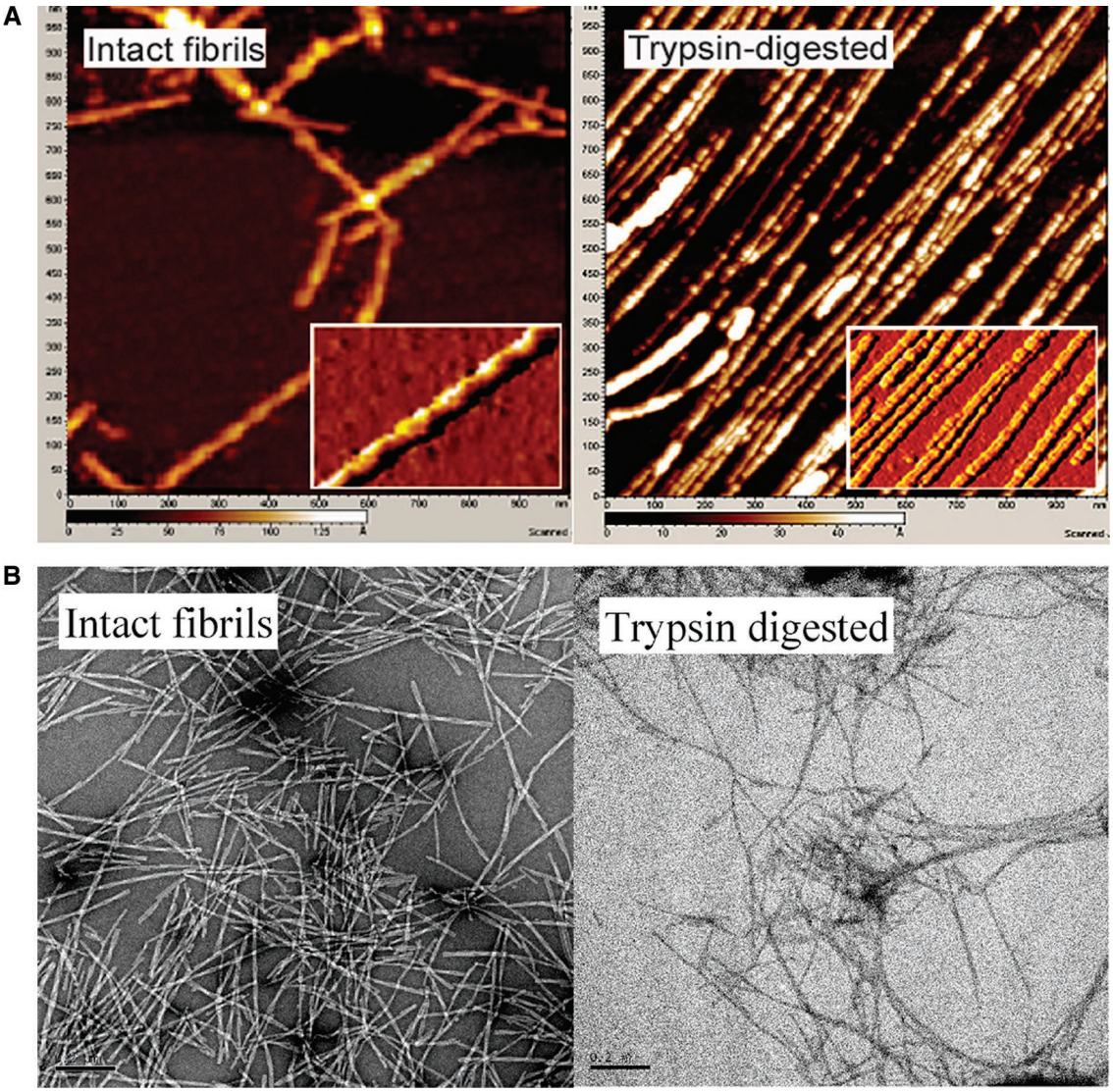

FIGURE 3: Atomic force and transmission electron microscopy images of α-synuclein fibrils after digestion by trypsin compared to intact fibrils. A. AFM: The intact α-synuclein fibrils show double-filament (protofibril) twisted morphology with a height of 136.2 ± 6.5 Å. The trypsin-digested fibrils show much thinner morphology with a height of 27.5 ± 1.6 Å. The inserted panels show the second derivative images of a single fibril, in which the double-filament twist (intact fibrils) and single filament (trypsin-digested fibrils) are more readily observed. B: TEM.

Table 2: Sizes of Different Kinds of Fibrils Measured from AFM

fibrils	size (Å)
full length	136.2 ± 6.5
trypsin digested	27.5 ± 1.6
syn30−103	28.8 ± 3.0
syn1−103	57.3 ± 3.3
syn30−140	107.7 ± 5.6

give the detailed structure of these fibrils, showing clearly that the fibril is a twisted double filament. The average height of these fibrils is 107.7 ± 5.6 Å, as expected a little smaller than that of intact fibrils of α-synuclein. However, the height of the fibrils from syn1−103 is much less than that of intact and N-terminal truncated fibrils, with an average height of 57.3 ± 3.3 Å. This diameter is a little less than half of the diameters of the other two fibrils. Interestingly, the fibrils from this C-terminal truncated protein also show a twisted pattern as shown in the detailed images in the insets to Figure 4. In marked contrast to all the other fibrils, the height of the fibrils grown from the double-truncated syn30−103 was only 28.8 ± 3.1 Å. This height is similar to that of the trypsin-digested resistant fibril core, smaller than one-fourth that of intact and N-terminal truncated fibrils, and half of that of the C-terminal truncated fibrils. The detailed images show a single smooth protofilament.

DISCUSSION

Hierarchical Structure of α-Synuclein Fibrils. The morphologies of endogenous fibrous proteins show that most of these insoluble proteins are assembled from a number of filaments (e.g. collagen is composed of three α-helical filaments; myosin fibrils contain two twisted filaments; the α-keratin of hair is a two-filament coiled coil). Interestingly, most pathological amyloid proteins also show multifilament (protofibrillar) assembly, as reported for Alzheimer's disease Aβ (*33*, *34*); α-synuclein, insulin, the B1 domain of protein G, and amyloidogenic Ig light chain (*32*). For the fibrous proteins, it is easy to understand that their structures are adapted for a biological function (i.e., strength, elasticity, mobility). In the case of amyloid fibrils it is less clear why they should be composed of multiple filaments: presumably

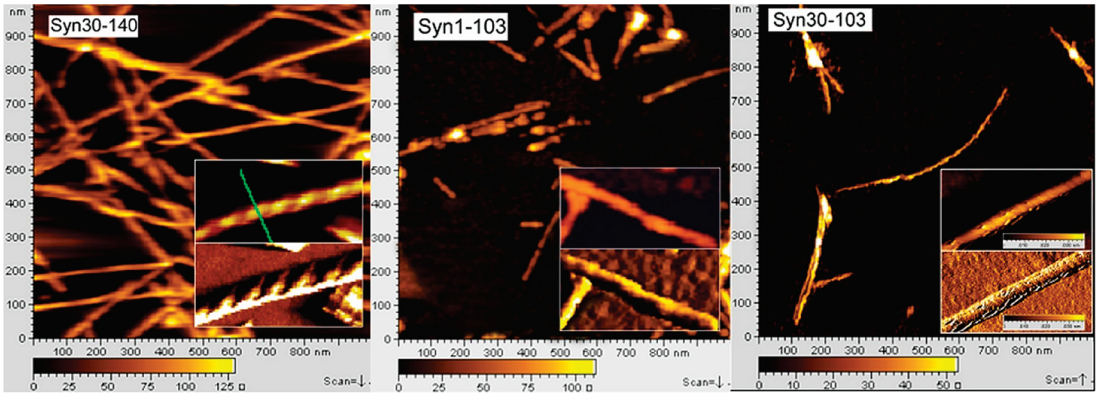

FIGURE 4: Morphology of the fibrils derived from three truncated α-synucleins. The inserted panels in each AFM image are a single fibril (upper) and its second derivative image (lower). Syn30−140 fibrils show long, straight morphology, and the double-filament twisted structure is observed in the enlarged fibril and its second derivative images (attributed to a pair of twisted protofibrils). Syn1−103 gives much thinner fibrils, but double-filament twisted structure is also observed (attributed to a protofibril consisting of two protofilaments). Syn30−103, however, shows very thin fibrils with a single filament and untwisted structure (attributed to a protofilament). The sizes of the three different fibrils are summarized in Table 2.

this reflects attractive interactions between the surface of the component protofilaments/protofibrils.

Previous investigations have shown that full-length mature fibrils of α-synuclein consist of four intertwined protofilaments (*32*) and have suggested that the fibril core consists of the central ~70 amino acids (*26*−*29*), consistent with a recent prediction (*35*). AFM investigations of full-length α-synuclein show a hierarchical assembly mechanism, with initial formation of protofilaments, two of which interact to form a protofibril, and two protofibrils assemble into mature fibrils (*32*). Different morphologies of α-synuclein aggregates have been reported depending on experimental conditions, especially pH (*36*, *37*). The potentially important role of the C-terminal region of α-synuclein in fibril formation has been attributed to negative charges in the 100−115 residue region (*38*).

The morphology and size of the various fibrils grown from the different lengths of α-synuclein studied in the present work are schematically represented in Figure 5. We assume that the height measured in the AFM images corresponds to the diameter of the fibrils. Both fibrils grown from full-length α-synuclein and the fibrils from syn30−140 are twisted, double-filaments: the ~30% decrease in diameter of the N-terminal truncated syn30−140 is attributed to the removal of the N-terminal 29 residues. Taking into consideration the difference in the length of the two proteins, we conclude that both of these two types of fibrils have the same hierarchical structure. In contrast, the syn1−103 fibrils have an average height close to half of that of the intact and N-terminal truncated fibrils: the removal of the C-terminal 37 residues alone cannot explain this large decrease in diameter. Instead, the size of the syn1−103 fibrils is very consistent with the size of a single protofibril (*32*). The formation of protofibrils, instead of the "mature" fibrils that full-length and N-terminal truncated α-synuclein formed, indicates that the C-terminal segment is necessary for the assembly of two protofibrils into a mature fibril. This is rather surprising, since the C-terminal region is not part of the fibril core, and is highly negatively charged. Since the protofibrils consist of two twisted protofilaments, the stabilizing intermolecular interactions between the two protofilaments does not involve the C-terminal region of the protein. In contrast, protofibrils were not formed by syn30−103; instead, this

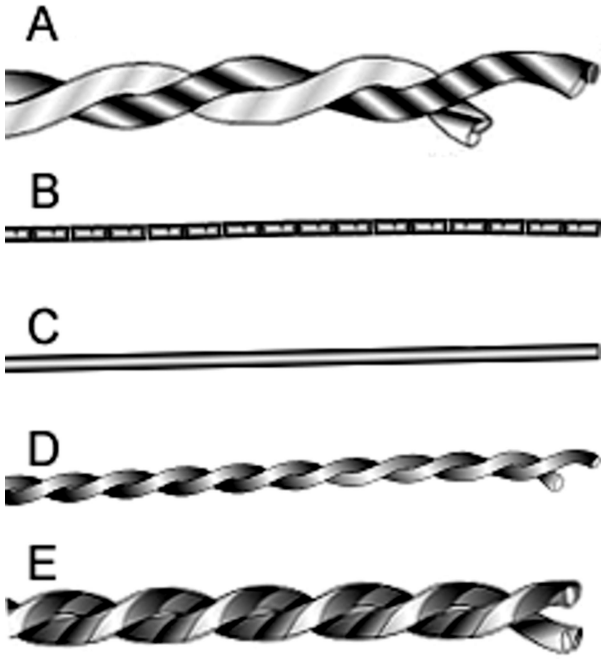

FIGURE 5: Schematic model of the size and morphology of the fibrils derived from three different truncated α-synucleins. A, fibril of full-length α-synuclein. The fibrils are composed of two twisted protofibrils, each in turn, consisting of two twisted protofilaments. B, trypsin-digested fibril. Because of the removal of the N- and C-terminal fragments, the mature fibril disassociated into a single, nontwisted filament. C, fibril derived from syn30−103 (a protofilament). D, fibril grown from syn1−103. Removal of the C-terminal fragment of α-synuclein inhibited its assembly to mature fibrils. Instead, the fibril from this truncated protein is composed of two twisted protofilaments, i.e., a protofibril. E, fibril from syn30−140, an N-terminal truncated protein. It is similar in morphology to a mature fibril from intact α-synuclein, but smaller due to the removal of the N-terminal fragment.

double-truncated α-synuclein formed a much thinner class of fibrils with average diameter of 29 Å, half the diameter of the protofibrils. We attribute this thinner fibril to a single protofilament, the basic element for fibril assembly. Interestingly, the size of these protofilaments is the same as the size of the fibril remnants from limited trypsin digestion of the intact fibrils. This suggests that even the well-packed fibrils of full-length α-synuclein, once their two terminal segments are removed, disassociate into protofilaments. These results

indicate that as long as either the N- or C-terminal region is present two protofilaments can form a protofibril. The proteolysis results indicate that once the proteases remove the exposed N- and C-terminal regions that are exposed in the mature fibrils (four twisted protofilaments) the fibrils begin to unravel so that the regions that lie within the interfaces between protofilaments (and protofibrils) become accessible to the proteases. It is interesting to note that the main fragment of the digestion was 1−102 from the MS analysis, but the morphology from AFM is different from that of the 1−103 mutant fragment. We believe that this is due to the difference between growing the fibrils from monomer vs digesting them from fully assembled fibrils.

Our observations are consistent with the hierarchical model for assembly of mature fibrils of α-synuclein. The basic structure of the fibrils is the protofilament, a single smooth filament directly assembled from individual α-synuclein molecules. Two protofilaments intertwine into a protofibril via interactions from the core residues and at least one of the terminal regions; then two protofibrils twist into mature fibrils via interactions involving the C-terminal region.

Arrangement of Molecules in Protofilaments. The way in which α-synuclein molecules assemble into protofilaments is still not understood. Analysis of several amyloid fibrils from short proteins/fragments and designed peptides, such as Alzheimer's Aβ (full length and its fragments) as well as other short peptides (*39*−*41*) using site-directed spin labeling (*42*), solid-state NMR (*43*, *44*), and X-ray diffraction (*34*, *40*, *40*, *41*, *45*−*51*), are consistent with a model of cross-β structure. In this model the β-strands run orthogonal to the fibril direction and are hydrogen-bonded, 4.7 Å apart, to form β-sheets parallel to the axis of the fibril. X-ray and electron diffraction studies of α-synuclein fibrils show a similar structure (*21*). For short peptides the arrangement of the molecules perpendicular to the fibril axis may be fully extended (*52*), or, in larger peptides such as Alzheimer's Aβ, include a hairpin loop (*45*, *53*−*55*). Recently, Eisenberg and co-workers have proposed eight classes of steric zippers, in which the β-strands differ in their arrangement with respect to orientation of their faces, direction, and whether parallel or antiparallel (*40*).

Given the 3.5 Å axial distances between adjacent amino acids in an extended β-strand, the length of the β-strands of α-synuclein calculated in this way exceeds the narrowest fiber dimension (*21*). Thus, a model of the arrangement of α-synuclein molecules with several turns and bend or loop regions was proposed (*26*). In the present study, we observed the smallest cross dimension of protofilaments to be ∼28 Å from both protease-resistant filaments of trypsin digested fibrils and the protofilaments derived from syn30−103. A potential model for α-synuclein protofilaments can be proposed, given that the protofilament assembled from a polypeptide of ∼70 amino acid residues, assuming 3.5 Å axial distances between adjacent amino acids in an extended β-strand, with 4.8 Å for the interstrand distance in a β-sheet, and that the length of the β-strands should not exceed eight amino acids (connected by β-turns), and the maximum number of strands would be seven, assuming all the strands are arranged in a β-sheet plane which in turn assemble into fibrils in-register, although we cannot eliminate the possibility that there are only five or six strands. The model is shown in Figure 6, with five strands for clarity. Thus, we propose

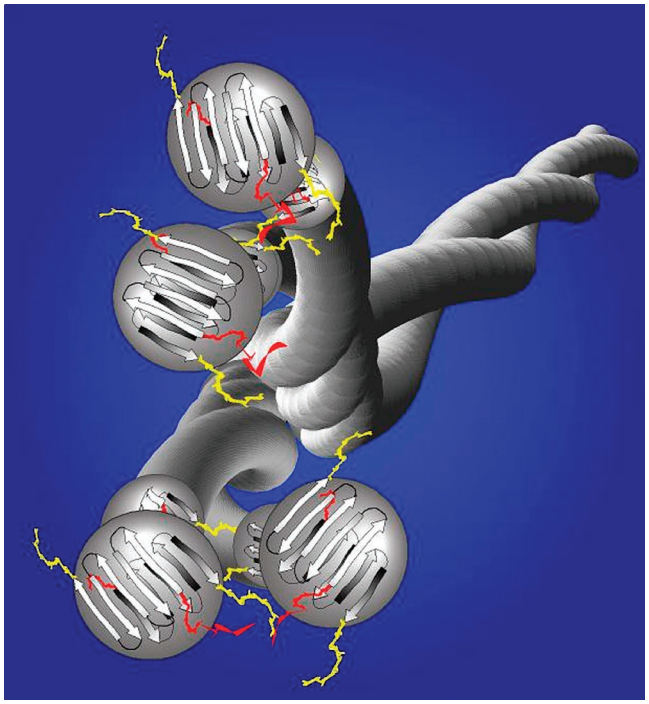

FIGURE 6: Model of the hierarchical structure and the roles of the terminal regions in the assembly of a α-synuclein fibril. Two protofilaments are shown interacting via their N- and/or C-terminal regions to form a protofibril. Subsequently, two protofibrils assemble by the interaction of C-terminal fragments to form a mature fibril.

that the fibrillar core of the protofilaments of α-synuclein consist of two β-sheets in which the β-strands are connected by β-turns with seven strands per molecule. From FTIR data, the major β-sheet component in the amide I band is around 1635 cm^{-1}, most consistent with parallel β-sheets.

Roles of Two Terminal Regions in Fibril Assembly. Interestingly, although the two terminal regions of α-synuclein were not found to be involved in the assembly of the core of protofilaments, they do participate in the assembly of the fibrils. As discussed above, the mature fibrils grown from full-length α-synuclein have a characteristic double−double-twisted pattern of structure, composed of four protofilaments. The protease-resistant core of the trypsin-digested fibrils shows only single filaments, characteristic in morphology of the protofilaments. This observation provides strong evidence that the terminal regions, either N- or C-terminal, or both, interact to hold the double−double-twisted assembly together. Furthermore, the mutant truncated proteins with selective removal of the N-, C-, or both termini allow us to assign a role to each terminal region in amyloidogenesis. Not surprisingly, the fibrils grown from syn30−103 exhibit the morphology of a single protofilament. This observation leads to the deduction that the absence of the two terminal regions results in failure to form mature fibrils because of the inability of protofilaments to self-interact. However, if the proteins are truncated at their N-terminal region only, the resulting peptide can still form mature fibrils, indicating that the N-terminal region is not essential for assembly of the mature fibrils. In contrast, the C-terminal-truncated proteins could not assemble into mature fibrils. This suggests that the C-terminal region plays a key role in the interaction between two protofibrils. The inability to form the two-protofilament twisted protofibrils in the absence of the

N-terminal region indicates that the N-terminal region is required for the interaction of two protofilaments to form a protofibril. Thus, both N- and C-terminal regions are involved in the interactions leading to mature fibril assembly. Interactions between the C-terminal region and the fibrillar core can be attributed to electrostatic interactions between the negatively charged C-terminus and the positively charged repeats in the core. The N-terminal interactions with the fibrillar core may arise from a combination of both hydrophobic and electrostatic interactions.

REFERENCES

1. Trojanowski, J. Q., and Lee, V. M. (2003) Parkinson's disease and related alpha-synucleinopathies are brain amyloidoses, *Ann. N. Y. Acad. Sci. 991*, 107−110.
2. Spillantini, M. G., Crowther, R. A., Jakes, R., Hasegawa, M., and Goedert, M. (1998) alpha-Synuclein in filamentous inclusions of Lewy bodies from Parkinson's disease and dementia with lewy bodies, *Proc. Natl. Acad. Sci. U.S.A. 95*, 6469−6473.
3. Kruger, R., Kuhn, W., Muller, T., Woitalla, D., Graeber, M., Kosel, S., Przuntek, H., Epplen, J. T., Schols, L., and Riess, O. (1998) Ala30Pro mutation in the gene encoding alpha-synuclein in Parkinson's disease, *Nat. Genet. 18*, 106−108.
4. Polymeropoulos, M. H., Lavedan, C., Leroy, E., Ide, S. E., Dehejia, A., Dutra, A., Pike, B., Root, H., Rubenstein, J., Boyer, R., Stenroos, E. S., Chandrasekharappa, S., Athanassiadou, A., Papapetropoulos, T., Johnson, W. G., Lazzarini, A. M., Duvoisin, R. C., Di Iorio, G., Golbe, L. I., and Nussbaum, R. L. (1997) Mutation in the alpha-synuclein gene identified in families with Parkinson's disease, *Science 276*, 2045−2047.
5. Zarranz, J. J., Alegre, J., Gomez-Esteban, J. C., Lezcano, E., Ros, R., Ampuero, I., Vidal, L., Hoenicka, J., Rodriguez, O., Atares, B., Llorens, V., Gomez, T. E., del Ser, T., Munoz, D. G., and de Yebenes, J. G. (2004) The new mutation, E46K, of alpha-synuclein causes Parkinson and Lewy body dementia, *Ann. Neurol. 55*, 164−173.
6. Singleton, A. B., Farrer, M., Johnson, J., Singleton, A., Hague, S., Kachergus, J., Hulihan, M., Peuralinna, T., Dutra, A., Nussbaum, R., Lincoln, S., Crawley, A., Hanson, M., Maraganore, D., Adler, C., Cookson, M. R., Muenter, M., Baptista, M., Miller, D., Blancato, J., Hardy, J., and Gwinn-Hardy, K. (2003) alpha-Synuclein locus triplication causes Parkinson's disease, *Science 302*, 841.
7. Fuchs, J., Nilsson, C., Kachergus, J., Munz, M., Larsson, E. M., Schule, B., Langston, J. W., Middleton, F. A., Ross, O. A., Hulihan, M., Gasser, T., and Farrer, M. J. (2007) Phenotypic variation in a large Swedish pedigree due to SNCA duplication and triplication, *Neurology 68*, 916−922.
8. Chartier-Harlin, M. C., Kachergus, J., Roumier, C., Mouroux, V., Douay, X., Lincoln, S., Levecque, C., Larvor, L., Andrieux, J., Hulihan, M., Waucquier, N., Defebvre, L., Amouyel, P., Farrer, M., and Destee, A. (2004) Alpha-synuclein locus duplication as a cause of familial Parkinson's disease, *Lancet 364*, 1167−1169.
9. Ibanez, P., Bonnet, A. M., Debarges, B., Lohmann, E., Tison, F., Pollak, P., Agid, Y., Durr, A., and Brice, A. (2004) Causal relation between alpha-synuclein gene duplication and familial Parkinson's disease, *Lancet 364*, 1169−1171.
10. Miller, D. W., Hague, S. M., Clarimon, J., Baptista, M., Gwinn-Hardy, K., Cookson, M. R., and Singleton, A. B. (2004) Alpha-synuclein in blood and brain from familial Parkinson disease with SNCA locus triplication, *Neurology 62*, 1835−1838.
11. Masliah, E., Rockenstein, E., Veinbergs, I., Mallory, M., Hashimoto, M., Takeda, A., Sagara, Y., Sisk, A., and Mucke, L. (2000) Dopaminergic loss and inclusion body formation in alpha-synuclein mice: implications for neurodegenerative disorders, *Science 287*, 1265−1269.
12. van Der, P. H., Wiederhold, K. H., Probst, A., Barbieri, S., Mistl, C., Danner, S., Kauffmann, S., Hofele, K., Spooren, W. P., Ruegg, M. A., Lin, S., Caroni, P., Sommer, B., Tolnay, M., and Bilbe, G. (2000) Neuropathology in mice expressing human alpha-synuclein, *J. Neurosci. 20*, 6021−6029.
13. Feany, M. B., and Bender, W. W. (2000) A Drosophila model of Parkinson's disease, *Nature 404*, 394−398.
14. Weinreb, P. H., Zhen, W., Poon, A. W., Conway, K. A., and Lansbury, P. T., Jr. (1996) NACP, a protein implicated in Alzheimer's disease and learning, is natively unfolded, *Biochemistry 35*, 13709−13715.
15. Uversky, V. N., Gillespie, J. R., and Fink, A. L. (2000) Why are "natively unfolded" proteins unstructured under physiologic conditions?, *Proteins 41*, 415−427.
16. Dedmon, M. M., Lindorff-Larsen, K., Christodoulou, J., Vendruscolo, M., and Dobson, C. M. (2005) Mapping Long-Range Interactions in alpha-Synuclein using Spin-Label NMR and Ensemble Molecular Dynamics Simulations, *J. Am. Chem. Soc. 127*, 476−477.
17. Eliezer, D., Kutluay, E., Bussell, R., Jr., and Browne, G. (2001) Conformational properties of alpha-synuclein in its free and lipid-associated states, *J. Mol. Biol. 307*, 1061−1073.
18. Davidson, W. S., Jonas, A., Clayton, D. F., and George, J. M. (1998) Stabilization of alpha-synuclein secondary structure upon binding to synthetic membranes, *J. Biol. Chem. 273*, 9443−9449.
19. Jo, E., McLaurin, J., Yip, C. M., George-Hyslop, P., and Fraser, P. E. (2000) alpha-Synuclein membrane interactions and lipid specificity, *J Biol. Chem 275*, 34328−34334.
20. Conway, K. A., Harper, J. D., and Lansbury, P. T., Jr. (2000) Fibrils formed in vitro from alpha-synuclein and two mutant forms linked to Parkinson's disease are typical amyloid, *Biochemistry 39*, 2552−2563.
21. Serpell, L. C., Berriman, J., Jakes, R., Goedert, M., and Crowther, R. A. (2000) Fiber diffraction of synthetic alpha-synuclein filaments shows amyloid-like cross-beta conformation, *Proc. Natl. Acad. Sci. U.S.A. 97*, 4897−4902.
22. Iwai, A., Yoshimoto, M., Masliah, E., and Saitoh, T. (1995) Non-A beta component of Alzheimer's disease amyloid (NAC) is amyloidogenic, *Biochemistry 34*, 10139−10145.
23. Ueda, K., Fukushima, H., Masliah, E., Xia, Y., Iwai, A., Yoshimoto, M., Otero, D. A., Kondo, J., Ihara, Y., and Saitoh, T. (1993) Molecular cloning of cDNA encoding an unrecognized component of amyloid in Alzheimer disease, *Proc. Natl. Acad. Sci. U.S.A. 90*, 11282−11286.
24. Giasson, B. I., Murray, I. V., Trojanowski, J. Q., and Lee, V. M. (2001) A hydrophobic stretch of 12 amino acid residues in the middle of alpha- synuclein is essential for filament assembly, *J. Biol. Chem. 276*, 2380−2386.
25. Uversky, V. N., and Fink, A. L. (2002) Amino acid determinants of alpha-synuclein aggregation: putting together pieces of the puzzle, *FEBS Lett. 522*, 9−13.
26. Der-Sarkissian, A., Jao, C. C., Chen, J., and Langen, R. (2003) Structural organization of alpha-synuclein fibrils studied by site-directed spin labeling, *J. Biol. Chem. 278*, 37530−37535.
27. Miake, H., Mizusawa, H., Iwatsubo, T., and Hasegawa, M. (2002) Biochemical characterization of the core structure of alpha-synuclein filaments, *J. Biol. Chem. 277*, 19213−19219.
28. Heise, H., Hoyer, W., Becker, S., Andronesi, O. C., Riedel, D., and Baldus, M. (2005) Molecular-level secondary structure, polymorphism, and dynamics of full-length {alpha}-synuclein fibrils studied by solid-state NMR, *Proc. Natl. Acad. Sci. U.S.A. 102*, 15871−15876.
29. Del, M. C., Greenbaum, E. A., Mayne, L., Englander, S. W., and Woods, V. L., Jr. (2005) Structure and properties of {alpha}-synuclein and other amyloids determined at the amino acid level, *Proc. Natl. Acad. Sci. U.S.A. 102*, 15477−15482.
30. Conway, K. A., Harper, J. D., and Lansbury, P. T. (1998) Accelerated in vitro fibril formation by a mutant *a*-synuclein linked to early-onset Parkinson disease, *Nat. Med. 4*, 1318−1320.
31. Naiki, H., Higuchi, K., Hosokawa, M., and Takeda, T. (1989) Fluorometric Determination of Amyloid Fibrils *in Vitro* Using the Fluorescent Dye, Thioflavin T, *Anal. Biochem. 177*, 244−249.
32. Khurana, R., Ionescu-Zanetti, C., pope, M., Li, J., Nielson, L., Ramirez-Alvarado, M., Regan, L., Fink, A. L., and Carter, S. A. (2003) A general model for amyloid fibril assembly based on morphological studies using atomic force microscopy, *Biophys. J. 85*, 1135−1144.
33. Harper, J. D., Lieber, C. M., and Lansbury, P. T., Jr. (1997) Atomic force microscopic imaging of seeded fibril formation and fibril branching by the Alzheimer's disease amyloid-beta protein, *Chem. Biol. 4*, 951−959.
34. Malinchik, S. B., Inouye, H., Szumowski, K. E., and Kirschner, D. A. (1998) Structural Analysis of Alzheimer's β(1−40) Amyloid: Protofilament Assembly of Tubular Fibrils, *Biophys. J. 74*, 422−429.
35. Zibaee, S., Makin, O. S., Goedert, M., and Serpell, L. C. (2007) A simple algorithm locates beta-strands in the amyloid fibril core

of alpha-synuclein, Abeta, and tau using the amino acid sequence alone, *Protein Sci. 16*, 906−918.
36. Hoyer, W., Antony, T., Cherny, D., Heim, G., Jovin, T. M., and Subramaniam, V. (2002) Dependence of alpha-synuclein aggregate morphology on solution conditions, *J. Mol. Biol. 322*, 383−393.
37. Hoyer, W., Cherny, D., Subramaniam, V., and Jovin, T. M. (2004) Rapid self-assembly of alpha-synuclein observed by in situ atomic force microscopy, *J. Mol. Biol. 340*, 127−139.
38. Murray, I. V., Giasson, B. I., Quinn, S. M., Koppaka, V., Axelsen, P. H., Ischiropoulos, H., Trojanowski, J. Q., and Lee, V. M. (2003) Role of alpha-Synuclein Carboxy-Terminus on Fibril Formation in Vitro, *Biochemistry 42*, 8530−8540.
39. Makin, O. S., and Serpell, L. C. (2005) Structures for amyloid fibrils, *FEBS J. 272*, 5950−5961.
40. Sawaya, M. R., Sambashivan, S., Nelson, R., Ivanova, M. I., Sievers, S. A., Apostol, M. I., Thompson, M. J., Balbirnie, M., Wiltzius, J. J., McFarlane, H. T., Madsen, A. O., Riekel, C., and Eisenberg, D. (2007) Atomic structures of amyloid cross-beta spines reveal varied steric zippers, *Nature 447*, 453−457.
41. Nelson, R., Sawaya, M. R., Balbirnie, M., Madsen, A. O., Riekel, C., Grothe, R., and Eisenberg, D. (2005) Structure of the cross-[beta] spine of amyloid-like fibrils, *Nature 435*, 773−778.
42. Torok, M., Milton, S., Kayed, R., Wu, P., McIntire, T., Glabe, C. G., and Langen, R. (2002) Structural and dynamic features of Alzheimer's Abeta peptide in amyloid fibrils studied by site-directed spin labeling, *J. Biol. Chem. 277*, 40810−40815.
43. Luhrs, T., Ritter, C., Adrian, M., Riek-Loher, D., Bohrmann, B., Dobeli, H., Schubert, D., and Riek, R. (2005) 3D structure of Alzheimer's amyloid-beta(1−42) fibrils, *Proc. Natl. Acad. Sci. U.S.A. 102*, 17342−17347.
44. Tycko, R. (2004) Progress towards a molecular-level structural understanding of amyloid fibrils, *Curr. Opin. Struct. Biol. 14*, 96−103.
45. Fraser, P. E., Nguyen, J. T., Inouye, H., Surewicz, W. K., Selkoe, D. J., Podlisny, M. B., and Kirschner, D. A. (1992) Fibril formation by primate, rodent, and Dutch-hemorrhagic analogues of Alzheimer amyloid beta-protein, *Biochemistry 31*, 10716−23.
46. Fraser, P. E., McLachlan, D. R., Surewicz, W. K., Mizzen, C. A., Snow, A. D., Nguyen, J. T., and Kirschner, D. A. (1994) Conformation and fibrillogenesis of Alzheimer A beta peptides with selected substitution of charged residues, *J. Mol. Biol. 244*, 64−73.
47. Halverson, K., Fraser, P. E., Kirschner, D. A., and Lansbury, P. T. (1990) Molecular determinants of amyloid deposition in Alzheimer's disease, *Biochemistry 29*, 2639−44.
48. Inouye, H., Fraser, P. E., and Kirschner, D. A. (1993) Structure of beta-crystallite assemblies formed by Alzheimer beta- amyloid protein analogues: analysis by x-ray diffraction, *Biophys. J. 64*, 502−519.
49. Inouye, H., and Kirschner, D. A. (1996) Refined fibril structures: the hydrophobic core in Alzheimer's amyloid beta-protein and prion as revealed by X-ray diffraction, *Ciba Found. Symp. 199*, 22−35.
50. Kirschner, D. A., Inouye, H., Duffy, L. K., Sinclair, A., Lind, M., and Selkoe, D. J. (1987) Synthetic peptide homologous to beta protein from Alzheimer disease forms amyloid-like fibrils in vitro, *Proc. Natl. Acad. Sci. U.S.A. 84*, 6953−6957.
51. Sikorski, P., Atkins, E. D., and Serpell, L. C. (2003) Structure and texture of fibrous crystals formed by Alzheimer's abeta(11−25) peptide fragment, *Structure. (Camb) 11*, 915−926.
52. Makin, O. S., Atkins, E., Sikorski, P., Johansson, J., and Serpell, L. C. (2005) Molecular basis for amyloid fibril formation and stability, *Proc. Natl. Acad. Sci. U.S.A. 102*, 315−320.
53. Paravastu, A. K., Petkova, A. T., and Tycko, R. (2006) Polymorphic fibril formation by residues 10−40 of the Alzheimer's beta-amyloid peptide, *Biophys. J. 90*, 4618−4629.
54. Hilbich, C., Kisterswoike, B., Reed, J., Masters, C. L., and Beyreuther, K. (1991) Aggregation and Secondary Structure of Synthetic Amyloid β-A4 Peptides of Alzheimers Disease, *J. Mol. Biol. 218*, 149−163.
55. Serpell, L. C., Blake, C. C., and Fraser, P. E. (2000) Molecular structure of a fibrillar Alzheimer's abeta fragment, *Biochemistry 39*, 13269−13275.

BI7014053